GEOPHYSICS, VOL. 82, NO. 3 (MAY-JUNE 2017); P. J1–J8, 8 FIGS.
10.1190/GEO2016-0364.1

Practical considerations in the use of edge detectors for geologic mapping using magnetic data

Mark Pilkington[1] and Victoria Tschirhart[1]

ABSTRACT

Locating the edges of magnetized sources provides a fundamental tool in the geologic interpretation of magnetic field data. Much recent effort has been expended on developing improvements to existing edge-detection methods, resulting in purported increases in accuracy and continuity along edges, reduction of noise effects, and limiting the influences of variable depth to source, magnetization direction, and source dip. These endeavors are valuable and provide interpreters with a wider range of tools to carry out geologic interpretations of aeromagnetic data. Nevertheless, survey parameters such as flight height and line spacing impose limits on the quality of edge locations that can be achieved. Using model studies, we quantify the effects that source size, depth, and interference between sources have on calculated edge locations. Based on the known behavior of established edge detectors, we found that many of the newer approaches offer limited advantages over older methods. Consequently, we studied an example of field mapping of geologic contacts in the Canadian Shield, supported by aeromagnetic data, using calculation of a standard edge detector: the horizontal gradient magnitude of the total magnetic field or TF-hgm. Calculated edge locations estimated from this method appear sufficiently accurate and continuous to provide a solid basis on which the mapping campaign was based and executed successfully.

INTRODUCTION

Determining the location of lateral magnetization contrasts, or equivalently, the edges of magnetized sources, is a fundamental tool in the geologic interpretation of magnetic data. Mapping these edges is akin to constructing a geologic map consisting of units of similar lithologies, whose boundaries are defined as geologic contacts. For magnetic data, the presence of a lateral change in magnetization might not be caused only by a change in lithology, but it can also have a structural, metamorphic, or mineralogical origin, and it can reflect the deformation and alteration history of the region. Nonetheless, delineating "edges" from magnetic data is a crucial step in mapping geologic units. In areas of overburden and extensive till cover, aeromagnetic data are essential for producing geologic maps. By examining the magnetic map, interpreters can trace continuous magnetic units between known outcrops based on calibrated correlations between anomaly character and lithology in areas where bedrock is well-exposed. In till-covered areas, the geologic map is often based predominately on interpretations of the aeromagnetic map and its derivative products along with satellite imagery; thus, accurately located edges are fundamental to the map-making process.

The existence of a large number of edge detectors (EDs) currently available indicates that no single ED is appropriate for every situation nor performs better than all others. Improving the performance of EDs requires the consideration of several points. Achieving greater accuracy, reduced interference, and independence from depth variations inevitably leads to operating in the higher frequency portion of the data spectrum in which signal-to-noise ratios are low. Reducing the effects of magnetization and dip also leads to coping with higher noise levels because EDs that are insensitive to these variables often involve both the vertical gradient and horizontal gradients, so they are more likely sensitive to noise. There is a well-known trade-off between accuracy and noise level. Even though noise and other unwanted field components can be present at low frequencies (e.g., regional field effects, survey compilation errors), for EDs, the focus is on the high-frequency end of the spectrum. The success of an ED will depend on where it is located on the trade-off curve between noise and accuracy. Where this point should be is influenced by the scale of investigation because for larger scales, higher frequencies are less important. It is also dependent on what the edges are used for, which will determine the level of accuracy we require. Mapping contacts favorable for mineralization requires high accuracy so that they can be effectively located in

Manuscript received by the Editor 8 July 2016; revised manuscript received 22 November 2016; published online 27 February 2017.
[1]Geological Survey of Canada, Ottawa, Ontario, Canada. E-mail: mark.pilkington@canada.ca; victoria.tschirhart@canada.ca.

the field from maps. Getting approximate contacts for subsequent modeling requires less accurate locations because the shapes of units and their interrelationships are more important. In a similar fashion, using marker horizons within a lithologic unit focuses on the patterns of these variations rather than requiring accurate contact locations.

Choosing the optimum point on the trade-off curve is also dependent on data quality, which is out of our control post acquisition. We can smooth the data, which moves the point down to lower noise and accuracy levels. Using an ED based on higher order derivatives means we are limited to very high quality data or we have to smooth the data and potentially remove the high-frequency signal originating from geologic sources. Conversely, for low-order derivative methods, especially those using only horizontal derivatives, we can cope with much lower quality data and still produce reliable edge locations. The final factor controlling accuracy is not related to the ED used but the survey specifications. Line spacing and more importantly survey height will determine the resolution of units possible, control the level of interference between adjacent sources, and set the limit on the degree of detail possible in any geologic interpretations based on edges.

EDGE DETECTORS

Although new methods of edge detection are constantly being developed, a few remain as standards that are used for comparison and as a baseline for judging any recent improvements. The established methods comprise the following: total field horizontal gradient magnitude (TF-hgm), analytic signal (AS), tilt angle (TI), tilt horizontal gradient magnitude (TI-hgm), local wavenumber (LW), theta angle (TH), pseudogravity horizontal gradient magnitude (PSG-hgm), and horizontal tilt angle (TDX). They have been discussed widely, and several comparisons have been carried out (Phillips, 2000; Fairhead et al., 2004; Pilkington and Keating, 2004, 2009; Fairhead and Williams, 2006; Li, 2006a). Even this relatively small number of EDs demonstrates that no single method has all the desirable properties of an effective mapper. The PSG-hgm (Cordell and Grauch, 1985) is stable, but it lacks resolution because it is based on the pseudogravity field, so it is one level of derivative below that of the magnetic field. It is also sensitive to magnetization direction and source-dip effects (Grauch and Cordell, 1987). Figure 1 shows the effect that the dip of a contact has on edge locations from several EDs. As the dip decreases, the edge locations migrate in the down-dip direction. The AS (Nabighian, 1972) and LW (Thurston and Smith, 1997) are, for 2D structures, not affected by dip or magnetization effects, but they are sensitive to noise and gridding, so they often suffer from poor continuity.

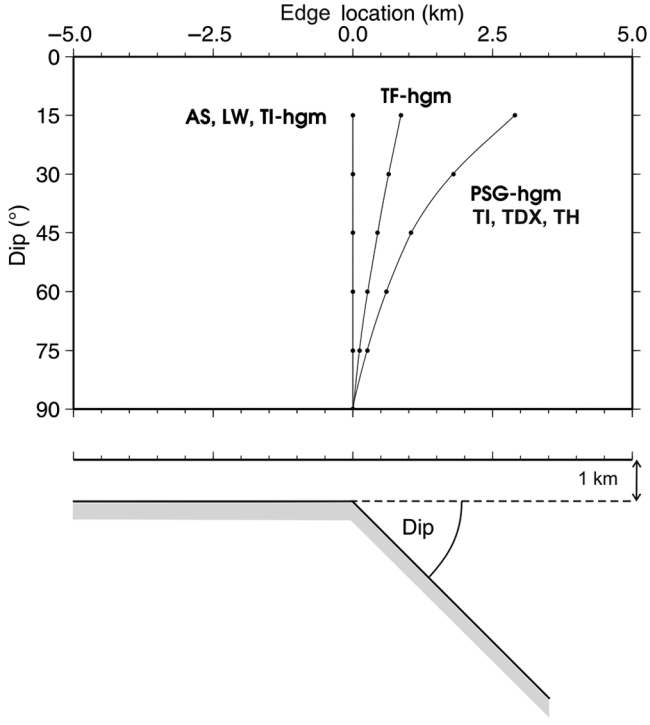

Figure 1. Edge locations for several edge detectors discussed in the text for a dipping contact. The contact edge is located horizontally at 0 km at a depth of 1 km. Magnetization and the inducing field are vertical. For example, the TF-hgm maximum is offset 0.625 km away from the true edge for a dip of 30°.

The TF-hgm (Phillips, 2000; Grauch et al., 2001), being based only on horizontal derivatives, is very stable in the presence of noise, but it is affected by dip and magnetization variations. The TI (Miller and Singh, 1994), TDX (Cooper and Cowan, 2006), and TH (Wijns et al., 2005) are related methods (Li, 2006b), and all are sensitive to dip and magnetization effects. The TI-hgm approach (Verduzco et al., 2004) is not influenced by dip or magnetization effects, but it tends to produce secondary edges. As expected, there exists a trade-off between stability and avoiding dip/magnetization effects. Similarly, EDs involving higher order derivatives will always be less effective in the presence of noise. Equally important are the redundancies that exist between different EDs, which show that different methods effectively produce the same result (Fairhead and Williams, 2006; Li, 2006b). For example, the TI, TDX, and TH methods all produce edge locations equivalent to the zero contour of the vertical derivative of the magnetic field.

For those EDs affected by the presence of nonvertical source magnetization, reduction to the pole (RTP) can be used to mitigate this effect. Using RTP will, nonetheless, only correct for the induced magnetization direction and any remanent magnetization in the direction of the present field. Furthermore, the RTP transformation has serious limitations when used at low magnetic latitudes. Phillips (2000) and Grauch et al. (2001) combine the TF-hgm edge detector with RTP to give their HGM-RTP method. Here, we keep the RTP operation separate, so that there can be a clear comparison between EDs that do not involve such a transformation.

Nevertheless, improvements to standard ED approaches are being developed and advertised to provide improvements over existing techniques. Since the comparison of EDs in Pilkington and Keating (2009) more than 20 papers have been published on improvements to existing methods. In view of such an abundance of techniques available, it is appropriate to revisit some practical considerations on the use of EDs for geologic mapping. We also discuss recent developments in the light of requirements of geologic mapping to evaluate their relevance. Finally, we document an example of geologic mapping in an area of extensive till cover that used EDs during and after field mapping campaigns to successfully produce bedrock maps.

Resolution and interference effects

Regardless of the properties of a given ED, its performance is governed by survey specifications — primarily the height of the sensor above ground. Assuming that measurements are on a horizontal

surface or at a smooth enough level that calculated derivatives are approximately true, the survey height limits the resolution of magnetization contrasts that can be detected. Increasing the derivative level can improve resolution but with a proportional increase in high-frequency noise. Higher order derivatives will also magnify any secondary edges present, producing more false contacts. The lack of resolution caused by the finite survey height results in not only losing the ability to distinguish closely spaced magnetization contrasts, which coalesce and give the appearance of a single edge, but also leads to errors in the location of contacts that can be resolved.

Figure 2 shows the behavior of several EDs over a thick body as a function of distance to source, i.e., survey height plus body depth. For this example, the body sides and the magnetization direction are vertical, so no dip or magnetization effects are present. When the body is wide enough, no interference between the sides is produced and all the EDs provide an accurate estimate of their location (for simplicity, only one side of the body is shown in Figure 2). As the survey height increases, or equivalently, the body depth increases, interference between the effects of both sides becomes measurable, causing errors in the calculated edge locations. For some EDs, the edge positions migrate away from the body edges, reflecting the broader anomalies as the height increases. For other EDs, the edge locations move inward over the body and merge together when the height/width ratio is large enough. Figure 2 can be used to estimate errors expected in mapping units of a given width from data collected at a certain height. For example, even though all the EDs can resolve body edges when height/width = 0.5, errors in the edge locations vary from 30% to 60% of the height. Similarly, specifying a survey height of 150 m and requiring errors <15 m (10% height) means that units must be, for example, >215 m wide for the TF-hgm method and >400 m for the LW approach.

The model in Figure 2 is a single isolated body, so only interference between edges within the same source is considered. For more realistic cases with multiple sources, the interference effects become more complicated. Figure 3 characterizes the effect of interference between neighboring sources for the simple case of two vertically sided and magnetized contacts. The edge locations are shown for the EDs considered in Figure 2 as a function of the separation between the sources, measured in terms of the distance to source. Only one edge location is plotted in Figure 3, for simplicity, because the behavior for the two edges is symmetric. The shaded area indicates the limit at which the two calculated edge locations merge to give one value, halfway between the sources. Similar to the Figure 2 case, there are two groups of EDs that migrate in the opposite direction as the separation between the two bodies increases. Contrary to the single body case, TI-hgm, LW, and AS locations now move away from the bodies rather than toward their centers and vice versa for the remaining EDs. Repeating earlier error estimates for the interference case shows that a 10% error for data acquired at 150 m requires a separation between bodies of, for example, 300 m for TF-hgm and approximately 550 m for LW. These distances are larger than for the resolution (single-body) case suggesting that interference effects are more likely to be encountered than resolution

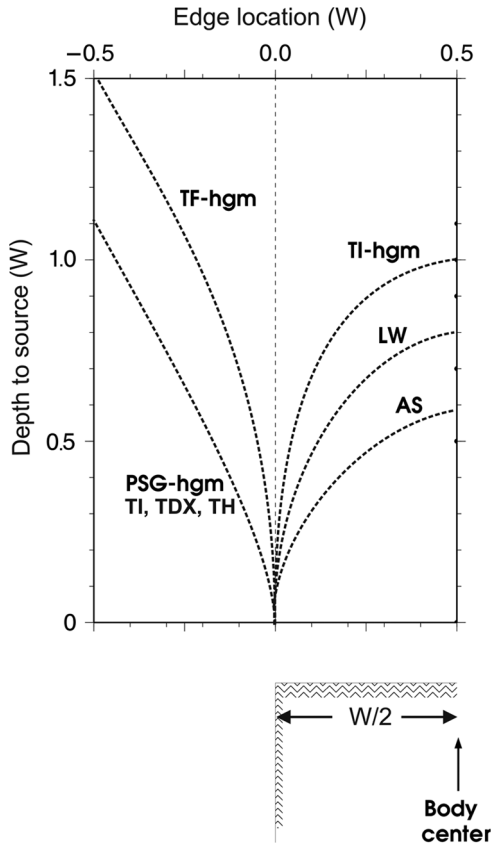

Figure 2. Edge locations for several edge detectors as a function of depth to source (after Pilkington, 2007). The dashed line indicates the body edge. Axes are scaled in terms of body width W.

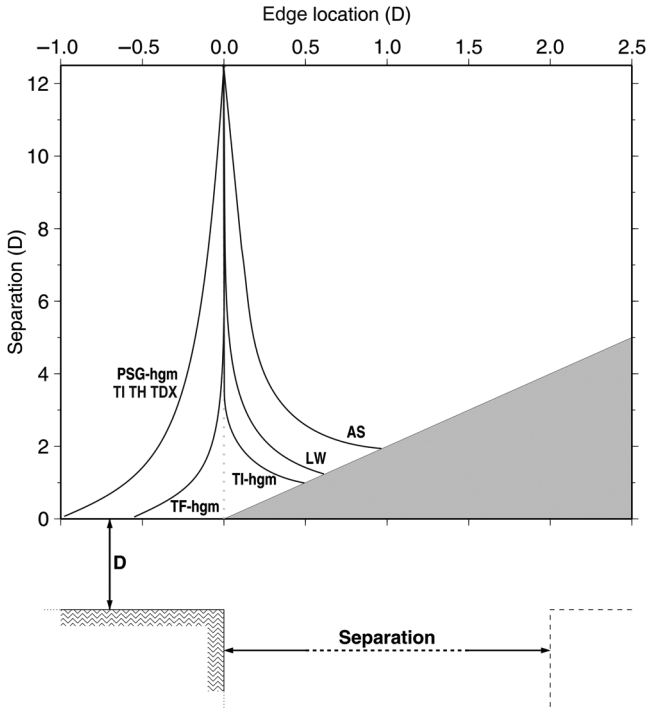

Figure 3. Edge locations for several EDs as a function of source separation (after Pilkington, 2007). The dashed line indicates the body edge location. Maxima are plotted for just one body because the maxima for the other body are simply mirror images of these locations. The shaded region indicates separation distances for which the two bodies are not resolved and only one maximum occurs. Axes are scaled in terms of body separation D.

effects. Figures 2 and 3 show that offsets for a given ED occur in different directions from the body edge, so the combination of small bodies placed at small intervals could result in the offset effects canceling each other and resulting in more reliable edge location estimates. But in real cases in which magnetized unit widths and the separation between them are variable, estimating errors using the above approaches is unlikely to be a realistic approach. Only where isolated units exist will some kind of error estimate be possible.

Clearly, errors in edge locations are likely to be significant as a result of resolution or interference effects for all EDs, the error being dependent on the ED used, and the specifics of the unit width and survey height. For geologic mapping applications in which airborne magnetic data are used, the separation between source and measurement means that these kinds of errors are most likely unavoidable.

Recent work

Recent improvements in edge detection have addressed several limitations that characterize existing EDs, such as those illustrated in Figures 2 and 3. The main focus of several new EDs is to improve the response from sources at different depths within a given data set. For deeper sources, the anomaly amplitude decrease may result in more subtle edge responses and the possibility of not detecting them. This has led to using "balanced" EDs, in which some kind of normalization is used to ensure that small- and large-amplitude responses are given equal weight. The tilt (TI) is the simplest balanced ED:

$$\mathrm{TI} = \tan^{-1}\left(\partial f/\partial z \,/\left[\left(\frac{\partial f}{\partial x}\right)^2 + \left(\frac{\partial f}{\partial y}\right)^2\right]\right), \qquad (1)$$

where f is the magnetic field. Here, the ratio of vertical to horizontal derivatives guarantees some independence of TI on the anomaly amplitude. Other balanced filters replace f in equation 1 with TF-hgm (Ferreira et al., 2013), AS (Cooper, 2014), or $\partial/\partial z$ (TF-hgm) (Zhang et al., 2015). For these cases, the use of different inputs to the tilt equation serves to balance the responses of the respective inputs. Balancing is also achieved by normalizing the responses within a specified window, similar to automatic gain control (Rajagopalan, 1987). Cooper and Cowan (2008) use the ratios of standard deviations of field derivatives, whereas Ma and Li (2012) use the maximum value of the TF-hgm within a window to normalize the response. Ma (2013) and Ma et al. (2014) combine the ratio and window approaches to balance a modified TDX expression, and they also introduce higher order derivatives to improve the resolution. Although detecting more edges, presumably due to deeper sources, can be advantageous, for surface geologic mapping applications, the focus is on outcropping sources. Hence, identifying deeper source edges is an unnecessary complication. Even with unbalanced EDs, low-amplitude anomalies due to buried sources may still be detected and mapped, particularly when maxima are being searched for quantitatively using a Blakely and Simpson (1986)-type method and not visually by an interpreter. Therefore, keeping deeper edge responses to a minimum is advantageous when mapping outcropping units.

Improving resolution has also been a goal with recently introduced EDs. For example, Wang et al. (2009) use the vertical derivative of the TF-hgm to sharpen the response over closely spaced sources. Other approaches also rely on using higher order derivatives, either of the field itself, which is then substituted into a standard ED formula such as TDX (Ma et al., 2016), or derived quantities, such as the AS (Yuan and Yu, 2015; Yao et al., 2016). Taking first-order derivatives of a stable ED such as TF-hgm might be a practical option because noise amplification is not expected to be severe for this case. However, using second- or third-order derivatives of the AS, which in its original form is already unstable in the presence of noise, is hardly recommended. Similarly, for EDs that produce secondary edges, although usually with small amplitudes, increasing the derivative level will just increase the likelihood of mapping spurious trends. All four methods mentioned above for improving resolution treat either gravity data or regional-scale magnetic data; hence, they allow for higher order derivatives to be calculated compared with lower altitude magnetic data containing a much greater level of high-frequency components.

Providing more edges using a new ED compared with the older methods is often presented as evidence of improved performance (Zhang et al., 2015; Sun et al., 2016). The new detail is usually not apparent throughout the data set, but it is restricted to small areas showing very finely detailed features. As such, these regions are at the limit of resolution for the ED and will be the most unreliable because of the greater likelihood of resolution and interference effects, which occur at small height/body-width ratios. By analogy to inverse problems in which we have more confidence in a solution that contains features produced by several methods, the case is similar for edges from several EDs. When one ED produces extra characteristics not reproducible with other methods, then its reliability should be questioned. This can be dealt with semiautomatically by using combinations of EDs (Cascone et al., 2012; Tschirhart and Morris, 2015).

Reducing the influence of noise is the aim of the normalized anisotropy variance edge method of Zhang et al. (2014), which is based on the balancing approach of Cooper (2009). Hidalgo-Gato and Barbosa (2015) use the monogenic signal to compute a lower order version of the tilt, which is less sensitive to noise, but it locates edges at the zero contours of the magnetic field rather than the zero value of the vertical gradient (Li and Pilkington, 2016). Finally, a useful goal of improving EDs is to reduce effects from nonvertical sources and/or magnetization. Cooper (2014) suggests that the tilt of the analytic signal improves the response over bodies in areas of low-inclination fields or having near-horizontal magnetizations. Using the tilt of the AS leads to a more balanced response, enhancing those edges that produce only low-amplitude analytic signal maxima. Nonetheless, the locations of edges based on maxima of the AS tilt remain unchanged compared with those from the AS.

An important gauge of improved mapping is the accuracy of the calculated edge locations. Inspection of the expressions for recently introduced EDs shows that in most cases, balancing does not influence the positions of the edges. Using the tilt of a given function such as the AS or TF-hgm does not alter the maxima locations (Ferreira et al., 2013; Cooper, 2014). Using a balancing factor in the denominator of several ED expressions preserves the location of the zero value of the vertical derivative used as an edge locator in Li et al. (2014) and Ma (2013). Similarly, normalizing values within a window will not affect edge locations (Wang et al., 2009; Ma and Li, 2012). On the other hand, those EDs using higher order vertical derivatives should provide a theoretical improvement (Ma et al., 2016; Yao et al., 2016) because the zero value of the vertical derivative approaches the body edge as the derivative order increases. However, for vertically sided and magnetized prisms, the location of the second vertical derivative zero value is only equal to the

maximum of the TF-hgm (Ma et al., 2016), and derivatives higher than second-order vertical derivatives are, in most cases, impractical to use.

In summary, many recently developed EDs offer limited advantages over older, more established EDs, such as those discussed in Figures 2 and 3. Edge locations either remain unchanged or their refinement is dependent on using higher order derivatives, causing increased noise corruption. Balancing existing EDs helps to equalize the response from sources at varying depths, but this does not provide an advantage when mapping surface geology, that is, sources from the shallowest depths. Finally, generating more fine detail in edge maps is often restricted to areas where resolution and interference effects are more likely present, calling into question any suggested information gained from such features. Consequently, the practical use of EDs for geologic mapping applications is outlined in the following using an established ED: the total field horizontal gradient magnitude.

RAE PROVINCE, CANADA

To illustrate the effectiveness of using edge detection during and after field mapping campaigns, we document an example from the Rae Province in Canada (Figure 4): specifically within the Montresor Belt (Percival et al., 2015). Similar Proterozoic supracrustal belts such as the Amer Belt are prospective for a variety of stratabound mineral deposits (Miller and LeCheminant, 1985; Tschirhart et al., 2015). Sandstone-hosted U and minor base-metal prospects have been identified by exploratory drilling and sampling of the magnetic Showing Lake Formation (upper Ps3; Figure 5) of the nearby Amer Group (Jefferson et al., 2015). Mineralized lenses are contained at several stratigraphic levels and strike 600–1525 m (Miller and LeCheminant, 1985). Within the Montresor Belt, a 4000 m-striking hydrothermal breccia zone with elevated levels of Cu, Ag, and Au is semiconcordant between stratigraphically higher and lower magnetic siltstone units (Figure 5 — triangle in unit Pmb). Undocumented stratabound U occurrences may similarly exist in the Montresor Ps3 sequence; however, the area has not been drilled or sampled for U occurrences. The stratiform nature of mineral occurrences and their association with magnetic marker units that occur within these belts emphasizes the importance of accurate contact locations for guiding future exploration efforts.

Located in the Rae Province that extends within Saskatchewan and Alberta through to Nunavut and the Northwest Territories, the Montresor Belt is part of the Rae cover sequence, which forms broad supracrustal belts unconformably overlying Archean crystalline basement (Figure 6; Rainbird et al., 2010). Within the belt Paleoproterozoic metasediments of the Montresor Group form a northeast–southwest-trending syncline overlying Archean granite and orthogneiss (Percival et al., 2015). The syncline is apparent in magnetic field data from the area (Figure 7). Because the TF-hgm edge detector is affected by nonvertical magnetization and dip (Figure 1), the magnetic field data were reduced to the pole to mitigate these effects. At such high latitudes (field inclination 84.6°), there is only a very small shift in the maxima locations as a result of pole reduction, not visible at the scale of Figure 7.

Heavy mineral beds in Ps3 siltstone sequences produce distinct linear magnetic highs of a few hundred nanotesla amplitude (Tschirhart et al., 2015). These marker units contain up to 2% magnetite in bands that also contain apatite, zircon, and tourmaline. With less than 5% outcrop, edge detection from the magnetic data is crucial for defining the upper and lower limits of sequences constrained by key magnetic marker units and constructing a geologic framework. Figure 8 shows a map of the TF-hgm calculated from the field in Figure 7. The maximum (edge) locations from the TF-ghm are given in Figure 7. The magnetic field data and derived TF-hgm ED images guided the map-making process (Percival et al., 2015). The vertical gradient and TI maps were also used, but only in a qualitative fashion to support the interpretation. Geologic units were mapped based on air photos, outcrop information, and the TF-hgm edge locations. The unconformity contact between Ps3 and Ps2 separates the prospective siltstone/sandstone unit (Ps3-Pms) from the schistose unit (Ps2-Pmp) or the underlying Archean crystalline basement (Agg). Within Ps3, two predominant magnetic marker horizons are present. The base of the lowermost magnetic horizon in Ps3 (Figure 5) stratigraphically defines the contact be-

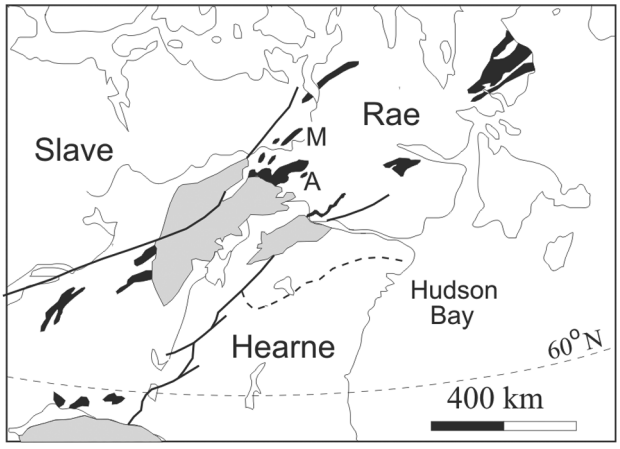

Figure 4. Location map of the Montresor Belt, Northwest Territories, Canada: M, Montresor Belt; A, Amer Belt; shaded areas, sedimentary basins; solid areas, supracrustal belts; and bold lines, major faults, shears.

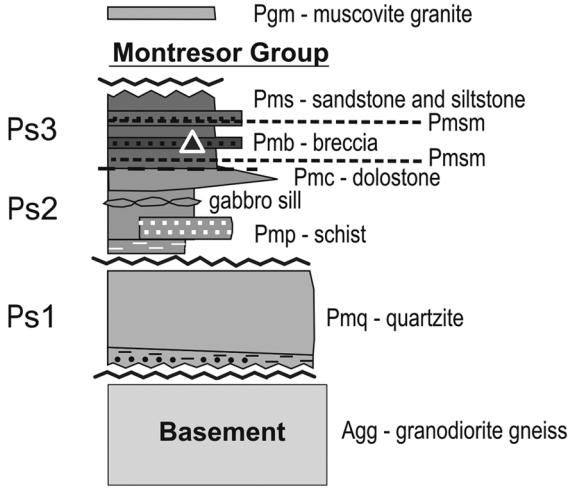

Figure 5. Stratigraphic column for the Montresor Belt. The Ps1-3 denotes stratigraphic sequences. Pgm, Pms, etc., denote lithologic units. Not all units are present in the study area. The age of Pgm unit is not known. Triangle, mineral occurrence; Pmsm, magnetic marker.

tween the Ps2 and Ps3 sequences. Marker horizons at higher levels in Ps3 (Pmsm) image crosscutting relationships and stratigraphic truncations, which provide structural constraints for reconstructing the tectonic history of the Montresor Belt (Tschirhart and Percival, 2016). The magnetic edge locations were also used in delineating sedimentary-igneous contacts such as those between the sandstone/siltstone units (Pms) and the more weakly magnetic muscovite granite (Pgm) and muscovite schist (Pmp) that together envelop the southwestern end of the syncline. The edges resulting from the contrast between the more magnetic Montresor sedimentary rocks and surrounding Archean gneiss (Agg) map the contact in the northwest of the study area. Some units were not mapped using the edge information, such as the block of brecciated intrusive rocks, Pmb (Figure 6) that was clearly identified from the well-exposed outcrop.

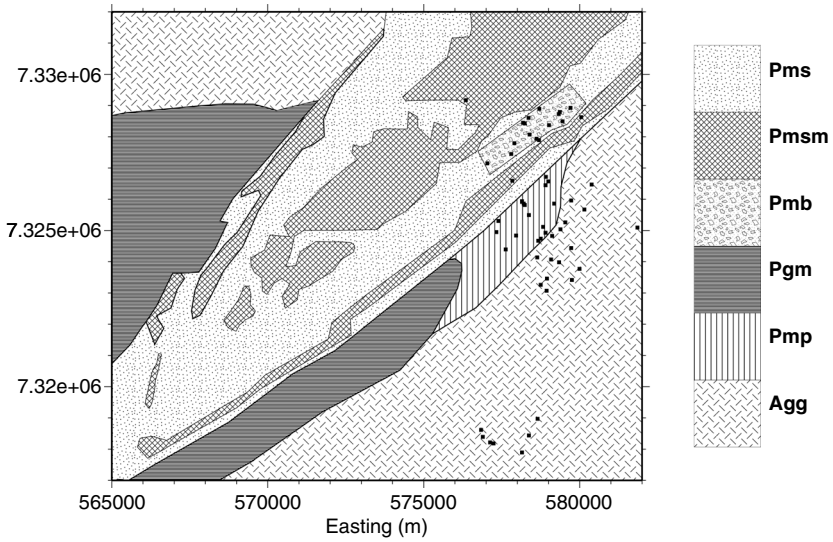

Figure 6. Geology of the Montresor study area (after Percival et al., 2015). The solid dots indicate outcrop locations sampled. See Figure 5 for an explanation of the rock type symbols.

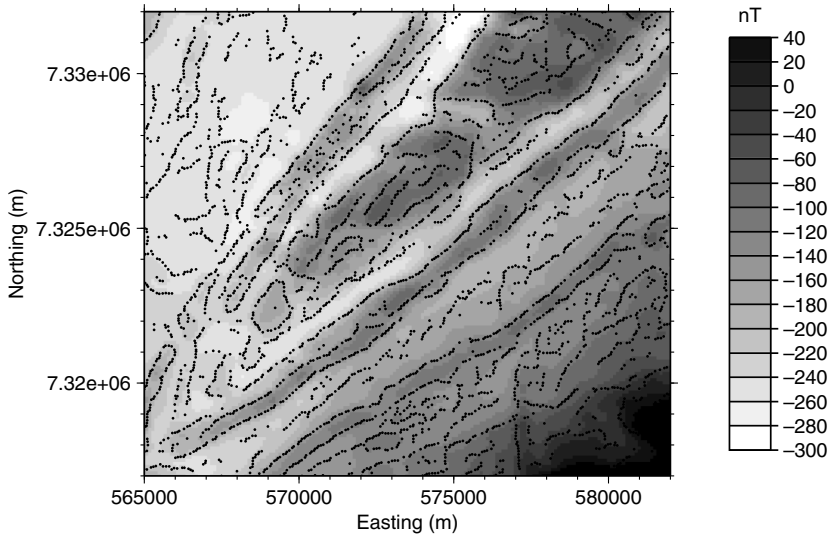

Figure 7. The RTP magnetic field for the Montresor study area. Edge locations from the horizontal gradient magnitude of the total magnetic field are superposed.

Not all edges are expected to be lithologic contacts. For example, the basement unit Agg is variably magnetized, and it produces edge trends with various orientations. The basement is mainly granodioritic, but it varies from granite to tonalite, so compositional effects will contribute to magnetization changes. Southeast of the syncline, some coherent edges in the basement trending northeast–southwest, parallel to the syncline axis, suggest a common deformation history. Observed dips within Ps3 in the mapped area in Figure 6 are 45°–60°, and Figure 1 would suggest approximately 35–70 m offsets (based on a 150 m flight height) down dip are possible for edges mapped with the TF-hgm as displayed in Figure 7. Resolution and interference effects are also present but depend on source widths and separations. In Figure 8, apparent values for these widths are mostly >300 m, which implies errors of <15 m (using Figures 2 and 3) in the positions of interpreted contacts. As well as providing lithologic contact information, the edge locations were used to constrain models of the southwest synclinal structure that hosts the hydrothermal breccia Pmb (Figure 6). The cross section of the syncline was initially modeled using magnetic susceptibility and dip measurements, where available, but ultimately the geometry of the northern limb, where fewer outcrop stations are located, was determined by modeling the magnetic anomalies. Available dip measurements for the southern limb provided primary constraints on the forward model, and they were in agreement with the geometry inferred from the magnetic data.

DISCUSSION

In the Montresor area, the edges mapped from magnetic data did not always correspond to lithologic contact locations, mainly due to variable magnetite concentration within Ps3 sedimentary sequences and gneissic basement units (Agg). Nonetheless, magnetic edges used in conjunction with outcrop information provided the basis for delineating major contacts, such as Ps2-Ps3. For strictly sedimentary sequences, usually characterized by low susceptibilities, only very small anomalies (<10 nT) would be expected to be mapped (Mørk et al., 2002). Depending on the bulk composition and oxidation state, metasedimentary rocks can be much more magnetic (McIntyre, 1980). Limited numbers of samples of equivalent units in the nearby Amer Belt (Figure 4) gave averages for the Ps1, Ps2, and Ps3 sequences of 0.008, 0.100, and 0.090×10^{-3} SI, respectively (Tschirhart et al., 2013), implying very small contrasts between these units. Consequently, the more magnetized marker horizons within the metasedimentary package (Figure 5) were crucial in aiding the mapping of lithologies and to constraining the form of the main synclinal structure of the belt. The edges from the markers in plan form clearly showed a symmetrical pattern indicative of a folded structure. Because the markers were observed in rock exposures (Figure 6), observed

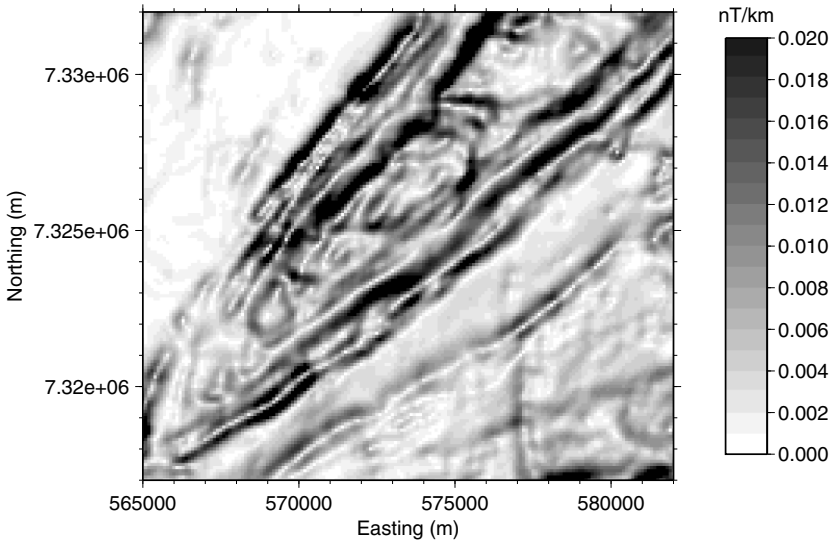

Figure 8. Horizontal gradient magnitude of the magnetic field for the Montresor study area.

lithologic contacts could then be extrapolated into covered areas based on the marker-related edges (Figure 7). As is often the case, most of the edges in Figure 7 are not explicitly incorporated into the final geologic map, but the trends provide guidance on placement of boundaries and structural features. From modeling studies, the spacing of apparent edge locations, and the measured dips, errors in the true edge positions are expected to be <100 m. The presence of multiple edges within units mapped from outcrop also suggests that the TF-hgm ED has sufficient resolving power to produce acceptable results for the magnetic data set used for analysis, so using a higher resolution ED would not necessarily provide a more reliable edge map. From the synthetic model studies in Figures 2 and 3, TF-hgm has the smallest offsets (between the mapped and true body edges) caused by resolution and interference effects, so it is expected to be reliable. Maxima offsets caused by source dip (and equivalently, magnetization) are also smaller for TF-hgm than most established EDs (Figure 1). The EDs not affected in 2D by dip or magnetization (AS, LW, and TI-hgm; Figure 1) are those most likely to be affected by noise, resolution, and interference effects. Because the study area is located at a highly magnetic latitude, the implemented RTP transformation is stable and the TF-hgm has the qualities of a reliable, stable, and accurate edge detector.

CONCLUSION

Unfortunately, in regional geologic mapping, a disconnect remains between ED products and their use by bedrock geologists. Quite often, if geophysical products are used, they are generally restricted to only display of a total magnetic field map or image and perhaps additionally a vertical gradient map or image. Accurate positioning of maxima locations corresponding to magnetization contrasts can still be done, but this requires knowledge of how anomalies are related to their sources in the region of interest, including the effects of source dip and strike. In contrast, an edge-location map can be produced with no prior knowledge of the geology required, and with little computational effort. It can then be added to the list of data sets that are assembled prior to the development of a final geologic map. A brief acquaintance with the limitations and behavior of a range of EDs, such as discussed earlier in this paper, would provide the necessary background for a meaningful interpretation to be made. The example outlined in the text demonstrates that the edge locations provided lithologic and structural information that constituted an invaluable contribution to the map-making process.

ACKNOWLEDGMENTS

The authors thank J. Percival and C. Jefferson for helpful discussions and M. Thomas for a thorough review that greatly improved the paper. The associate editor, M. Hidalgo-Gato and two anonymous reviewers provided numerous suggestions that have clarified several points. This work was done as part of Natural Resources Canada's Geo-Mapping for Energy and Minerals Program, Phase 2. This is Geological Survey of Canada Contribution 20160325.

REFERENCES

Blakely, R. J., and R. W. Simpson, 1986, Approximating edges of source bodies from magnetic or gravity anomalies: Geophysics, **51**, 1494–1498, doi: 10.1190/1.1442197.

Cascone, L., S. Campbell, C. Green, A. Salem, and D. Fairhead, 2012, ACLAS: A new automatic method of defining potential field lineaments using coherency analysis: 82nd Annual International Meeting, SEG, Expanded Abstracts, 1–6.

Cooper, G. R. J., 2009, Balancing images of potential field data: Geophysics, **74**, no. 3, L17–L20, doi: 10.1190/1.3096615.

Cooper, G. R. J., 2014, Reducing the dependence of the analytic signal amplitude of aeromagnetic data on the source vector direction: Geophysics, **79**, no. 4, J55–J60, doi: 10.1190/geo2013-0319.1.

Cooper, G. R. J., and D. R. Cowan, 2006, Enhancing potential field data using filters based on the local phase: Computers and Geosciences, **32**, 1585–1591, doi: 10.1016/j.cageo.2006.02.016.

Cooper, G. R. J., and D. R. Cowan, 2008, Edge enhancement of potential-field data using normalized statistics: Geophysics, **73**, no. 3, H1–H4, doi: 10.1190/1.2837309.

Cordell, L., and V. J. S. Grauch, 1985, Mapping basement magnetization zones from aeromagnetic data in the San Juan basin, New Mexico, *in* W. J. Hinze, ed., The utility of regional gravity and magnetic anomaly maps: SEG, 181–197.

Fairhead, J. D., and S. E. Williams, 2006, Evaluating normalized magnetic derivatives for structural mapping: 76th Annual International Meeting, SEG, Expanded Abstracts, 845–849.

Fairhead, J. D., S. E. Williams, and G. Flanagan, 2004, Testing magnetic local wavenumber depth estimation methods using a complex 3D test model: 74th Annual International Meeting, SEG, Expanded Abstracts, 742–745.

Ferreira, F. J. F., J. de Souza, A. B. e S. de Bongiolo, and L. G. de Castro, 2013, Enhancement of the total horizontal gradient of magnetic anomalies using the tilt angle: Geophysics, **78**, no. 3, J33–J41, doi: 10.1190/geo2011-0441.1.

Grauch, V. J. S., and L. Cordell, 1987, Limitations of determining density or magnetic boundaries from the horizontal gradient of gravity or pseudo-gravity data: Geophysics, **52**, 118–121, doi: 10.1190/1.1442236.

Grauch, V. J. S., M. R. Hudson, and S. A. Minor, 2001, Aeromagnetic expression of faults that offset basin fill, Albuquerque basin, New Mexico: Geophysics, **66**, 707–720, doi: 10.1190/1.1444961.

Hidalgo-Gato, M. C., and V. C. F. Barbosa, 2015, Edge detection of potential-field sources using scale-space monogenic signal: Fundamental principles: Geophysics, **80**, no. 5, J27–J36, doi: 10.1190/geo2015-0025.1.

Jefferson, C. W., J. C. White, G. M. Young, J. Patterson, V. Tschirhart, S. J. Pehrsson, L. Calhoun, R. H. Rainbird, T. Peterson, W. J. Davis, S. Tella, L. B. Chorlton, J. M. J. Scott, J. A. Percival, W. A. Morris, P. Keating, A. Anand, Y. Shelat, and D. MacIsaac, 2015, Outcrop and remote predictive geology of the Amer Belt and basement beside and beneath the northeast

Thelon Basin in parts of NTS 66A, B, C, F, G and H, Nunavut: Geological Survey of Canada, Open File 7242, 1 sheet.
Li, L., D. Huang, L. Han, and G. Ma, 2014, Optimised edge detection filters in the interpretation of potential field data: Exploration Geophysics, **45**, 171–176, doi: 10.1071/EG13059.
Li, X., 2006a, Understanding 3D analytic signal amplitude: Geophysics, **71**, no. 2, L13–L16, doi: 10.1190/1.2184367.
Li, X.., 2006b, On "Theta map: Edge detection in magnetic data" (C. Wijns, C. Perez, and P. Kowalczyk, 2005, GEOPHYSICS, 71, L39–L43): Geophysics, **71**, no. 3, X11, doi: 10.1190/1.2194525.
Li, X., and M. Pilkington, 2016, Attributes of the magnetic field, analytic signal and monogenic signal for gravity and magnetic interpretation: Geophysics, **81**, no. 6, J79–J86, doi: 10.1190/geo2015-0697.1.
Ma, G., 2013, Edge detection of potential field data using improved local phase filter: Exploration Geophysics, **44**, 36–41, doi: 10.1071/EG12022.
Ma, G., D. Huang, and C. Liu, 2016, Step-edge detection filters for the interpretation of potential field data: Pure and Applied Geophysics, **173**, 795–803, doi: 10.1007/s00024-015-1053-6.
Ma, G., and L. Li, 2012, Edge detection in potential fields with the normalized total horizontal derivative: Computers and Geosciences, **41**, 83–87, doi: 10.1016/j.cageo.2011.08.016.
Ma, G., C. Liu, and L. Li, 2014, Balanced horizontal derivative of potential field data to recognize the edges and estimate location parameters of the source: Journal of Applied Geophysics, **108**, 12–18, doi: 10.1016/j.jappgeo.2014.06.005.
McIntyre, J. I., 1980, Geological significance of magnetic patterns related to magnetite in sediments and metasediments: A review: Exploration Geophysics, **11**, 19–33, doi: 10.1071/EG980019.
Miller, A. R., and A. N. LeCheminant, 1985, Geology and uranium metallogeny of Proterozoic supracrustal successions, central District of Keewatin, N.W.T. with comparisons to northern Saskatchewan, *in* T. I. I. Sibbald, and W. Petruk, eds., Geology of uranium deposits: Canadian Institute of Mining and Metallurgy, 167–185.
Miller, H. G., and V. Singh, 1994, Potential field tilt: A new concept for location of potential field sources: Journal of Applied Geophysics, **32**, 213–217, doi: 10.1016/0926-9851(94)90022-1.
Mørk, M. B. E., S. A. McEnroe, and O. Olesen, 2002, Magnetic susceptibility of Mesozoic and Cenozoic sediments off mid Norway and the role of siderite: Implications for interpretation of high-resolution aeromagnetic anomalies: Marine and Petroleum Geology, **19**, 1115–1126, doi: 10.1016/S0264-8172(02)00115-0.
Nabighian, M. N., 1972, The analytic signal of two-dimensional magnetic bodies with polygonal cross-section: Its properties and use for automated anomaly interpretation: Geophysics, **37**, 507–517, doi: 10.1190/1.1440276.
Percival, J. A., V. Tschirhart, W. J. Davis, R. G. Berman, and A. Ford, 2015, Geology, Montresor River area, Nunavut, parts of NTS 66-H and NTS 66-I: Geological Survey of Canada, Canadian Geoscience Map 231 (preliminary) scale 1: 100 000.
Phillips, J., 2000, Locating magnetic contacts: A comparison of the horizontal gradient, analytic signal, and local wavenumber methods: 70th Annual International Meeting, SEG, Expanded Abstracts, 402–405.
Pilkington, M., 2007, Locating geologic contacts with magnitude transforms of magnetic data: Journal of Applied Geophysics, **63**, 80–89, doi: 10.1016/j.jappgeo.2007.06.001.
Pilkington, M., and P. B. Keating, 2004, Contact mapping from gridded magnetic data: A comparison of techniques: Exploration Geophysics, **35**, 306–311, doi: 10.1071/EG04306.
Pilkington, M., and P. B. Keating, 2009, The utility of potential field enhancements for remote predictive mapping: Canadian Journal of Remote Sensing, **35**, S1–S11, doi: 10.5589/m09-021.
Rainbird, R. H., W. J. Davis, S. J. Pehrsson, N. Wodicka, N. Rayner, and T. Skulski, 2010, Early Paleoproterozoic supracrustal assemblages of the Rae domain, Nunavut, Canada: Intracratonic basin development during supercontinent break-up and assembly: Precambrian Research, **181**, 167–186, doi: 10.1016/j.precamres.2010.06.005.
Rajagopalan, S., 1987, The use of 'automatic gain control' to display vertical magnetic gradient data: Exploration Geophysics, **18**, 166–169, doi: 10.1071/EG987166.
Sun, Y., W. Yang, X. Zeng, and Z. Zhang, 2016, Edge enhancement of potential field data using spectral moments: Geophysics, **81**, no. 1, G1–G11, doi: 10.1190/geo2014-0430.1.
Thurston, J. B., and R. S. Smith, 1997, Automatic conversion of magnetic data to depth, dip, and susceptibility contrast using the SPI method: Geophysics, **62**, 807–813, doi: 10.1190/1.1444190.
Tschirhart, P., and B. Morris, 2015, Improved edge detection mapping through stacking and integration: A case study in the Bathurst mining camp: Geophysical Prospecting, **63**, 283–295, doi: 10.1111/1365-2478.12188.
Tschirhart, V., W. A. Morris, C. W. Jefferson, P. Keating, J. C. White, and L. Calhoun, 2013, 3D geophysical inversion of the north-east Amer Belt and their relationship to geologic structure: Geophysical Prospecting, **61**, 547–560, doi: 10.1111/j.1365-2478.2012.01098.x.
Tschirhart, V., and J. A. Percival, 2016, Toward 3D structural constraints from magnetic models: An example from the Montresor belt, Nunavut, Canada: 25th Geophysical Conference, ASEG, Extended Abstracts, 898–900.
Tschirhart, V., J. A. Percival, and C. W. Jefferson, 2015, Geophysical models of the Montresor metasedimentary belt and its environs, central Nunavut, Canada: Canadian Journal of Earth Sciences, **52**, 833–845, doi: 10.1139/cjes-2015-0008.
Verduzco, B., J. D. Fairhead, C. M. Green, and C. MacKenzie, 2004, New insights to magnetic derivatives for structural mapping: The Leading Edge, **23**, 116–119, doi: 10.1190/1.1651454.
Wang, W., P. Yu, and Q. Zhiyun, 2009, A new edge recognition technology based on the normalized vertical derivative of the total horizontal derivative for potential field data: Applied Geophysics, **6**, 226–233, doi: 10.1007/s11770-009-0026-x.
Wijns, C., C. Perez, and P. Kowalczyk, 2005, Theta map: Edge detection in magnetic data: Geophysics, **70**, no. 4, L39–L43, doi: 10.1190/1.1988184.
Yao, Y., D. Huang, X. Yu, and B. Chai, 2016, Edge interpretation of potential field data with the normalized enhanced analytic signal: Acta Geodetica Geophysica, **51**, 125–136, doi: 10.1007/s40328-015-0120-x.
Yuan, Y., and Q. Yu, 2015, Edge detection in potential-field gradient tensor data by use of improved horizontal analytical signal methods: Pure and Applied Geophysics, **172**, 461–472, doi: 10.1007/s00024-014-0880-1.
Zhang, H. L., D. Ravat, Y. R. Marangoni, and X. Y. Hu, 2014, NAV-Edge: Edge detection of potential-field sources using normalized anisotropy variance: Geophysics, **79**, no. 3, J43–J53, doi: 10.1190/geo2013-0218.1.
Zhang, X., P. Yu, R. Tang, Y. Xiang, and C.-J. Zhao, 2015, Edge enhancement of potential field data using an enhanced tilt angle: Exploration Geophysics, **46**, 276–283, doi: 10.1071/EG13104.